Journal of Network Intelligence
Taiwan Ubiquitous Information
 ISSN 2414-8105
Volume **10**, Number **1**, February **2025**

Radio Frequency Electronic Communication Based on Artificial Intelligence Control System Optimization Design

Yu-Feng Zhao*

School of Electronics and IoT Engineering
Chongqing Industry Polytechnic College, Chongqing, 401120, P. R. China
zhaoyf@cqipc.edu.cn

Jie He

Lee Kong Chian Faculty of Engineering and Science
Tunku Abdul Rahman University, Kuala Lumpur 43000, Malaysia
hejie@cqipc.edu.cn

*Corresponding author: Yu-Feng Zhao
Received November 7, 2023, revised January 10, 2024, accepted March 15, 2024.

Abstract. *Traditional Radio Frequency (RF) electronic communication systems consume a lot of computing resources, and can gradually not meet people's requirements for efficient, fast and high-precision systems. For the purpose of accurately mapping the nonlinear relationship between input and output and solve the problem of RF electronic communication system, this paper designs an efficient RF electronic communication system by artificial intelligence control method. The system first preprocess the communication data, optimize the initial value of the data, and then train the neural network on the optimized data to achieve intelligent modeling, and then based on the model, the secondary superheterodyne receiving structure and the secondary frequency conversion transmission structure are used to separate the received optical signal into AC components for information decoding and DC components for energy harvesting, reduce crosstalk between RF signals, and ensure signal quality to improve the performance of the system. Simulation results show that compared with existing systems, the system designed in this paper has lower system gain flatness, modulation accuracy and power gain flatness.*
Keywords: radio frequency; electronic communication; artificial intelligence; neural network; information decoding

1. **Introduction.** As modern communication and Radio Frequency (RF) technology developing, RF circuits are gradually integrated, miniaturized in size and diversified in functions, resulting in higher and higher working frequencies of RF circuits and systems, making the research and design of communication systems more and more difficult. The traditional RF electronic communication system has a slow computing speed and consumes too many computing resources, which has gradually failed to meet people's requirements for efficient, fast and high-precision system [1,2,3]. Artificial intelligence methods developed by borrowing biological neurological properties have begun to attract attention and are gradually applied to the field of modeling of radio frequency electronic communication systems. Neurons are the basic building blocks of the ANN model, which can quickly and independently process information and store data information in each neuron. The entire neural network model is able to map nonlinear features and adapt

to changes with the environment, continuously learning to adjust the weights inside the network [4,5]. The modeling process of neural networks does not require knowledge of RF circuit expertise, and once the learning process is completed, the model can quickly and accurately map the nonlinear relationship between input and output, thereby solving the problems related to RF circuit modeling. It can be seen that intelligent neural network technology provides an effective solution to solve the problem of fast and accurate modeling of RF circuits.

1.1. **Related Work.** At present, artificial intelligence methods have distinctive characteristics and outstanding capabilities, and have been successfully applied to the field of radio frequency electronic communication, which has become a hot topic in the field of radio frequency electronic communication. For the purpose of continuously improving the accuracy of neural network models and shorting the training time of models, scholars have begun to research artificial intelligence technologies in related fields such as RF devices, antennas and model optimization. Rayas-Sanchez et al. [6] suggest a linear inverse spatial mapping RF microwave circuit optimization algorithm to realize the transient calculation of microwave circuit frequency domain and time domain. Compared with the traditional mapping method, the linear inverse spatial mapping method proposed in the literature can simplify the mapping difficulty and is suitable for the linear analysis model of RF circuit. Sen et al. [7], Chandrasekaran and Jordan [8] use neural network technology to extract parasitic parameters of integrated circuits. At the same time, a neural network model generated by automatic layout is also proposed to verify the extracted parasitic parameters. Kabir et al. [9] propose a microwave filter neural network model with multiple input variables. This method first decomposes the overall neural network into many neural network submodels, and then, the submodels are attached to empirical/equivalent models to obtain the final overall model. Compared with traditional neural network models, this method has higher accuracy, more input variables, and fewer sample sizes. In order to improve the accuracy of the model, Ko et al. [10] of Ohio State University proposed a field-effect transistor neural network model based on quasi-static measurement, which was validated using load line, output power, power efficiency, and load pull model. Tian et al. [11] and Srivastava et al. [12] used neural networks to establish a right-angle micro-coaxial bend of an RF microwave integrated circuit for design, so as to obtain a high-performance coaxial elbow, which is conducive to the design of folding micro-coaxial passive devices and miniaturizes the structure. while maintaining low losses and high matching. Inanlou et al. [13] used deep neural network technology to model the deep neural network of Doherty power amplifiers, using Relu Piecewise linear activation function, since the activation function derivative is constant, the gradient vanishing problem is controlled. Compared with the shallow neural network model of the traditional Doherty power amplifier, it can not only increase the output power of the margin call, but also overcome the complex memory effect of the power amplifier. Aiming at the dynamic nonlinear behavior of wideband RF power amplifiers, Kia [14] propose a deep neural network prediction model. This method first uses neural network, K nearest neighbor and other algorithms to process the copied signal, and then uses neural network technology to model, which can obtain better mean squared error and adjacent channel error power ratio. Lu et al. [15] propose a neural network model for reconfigurable microstrip antenna design optimization. In this method, the resonant frequency adjustment and return loss control are realized through the control circuit, so as to realize the design and optimization of the reconfigurable antenna. However, there are still many challenges to this method. Since the performance of AI models depends on sample data. The training speed depends on the sample data quality [16, 17, 18, 19]. If the quality of the sample data is low,

then the neural network training will require more sample data, resulting in longer time consumption and significantly less efficient modeling. Secondly, the research frequency is low and the scope is narrow. At present, the research of RF electronic communication systems based on artificial intelligence is generally concentrated in the circuits in the RF segment [20,21,22], and the more critical modeling methods of circuits and systems in the millimeter band still have many difficulties, resulting in the application of modeling methods in the millimeter wave band is rare, and the research results in this area are rarely reported.

1.2. **Motivation and contribution.** On behalf of promoting the application of artificial intelligence technology in the field of RF electronic communication system, this paper designs an optimized RF electronic communication system based on artificial intelligence neural network modeling technology. The system first combines data preprocessing, sample initial value optimization and neural network training and testing process to realize intelligent modeling functions, and then on the ground of the modeling model, adopts the secondary superheterodyne receiving structure and the secondary frequency conversion transmission structure, divides different modules according to the current, ensures the isolation between the modules, and reduces the crosstalk between RF signals. Simulation results imply that by selecting the appropriate parameter configuration to balance the performance between communication data transmission, the system designed in this paper can effectively improve the key performance of system gain flatness, modulation accuracy and power gain flatness.

2. Related theoretical knowledge.

2.1. **Data Preprocessing.** Data preprocessing, which is a method founded on data analysis technology [23], can process the original data, making the sample data easier to process and more representative, which is a very important step in the process of building artificial neural network models, but it is often regarded as a small problem and ignored. Assuming that the original sample data has m variables, the m variables can form 1 input m of the original sample data dimensional vectors $\boldsymbol{\gamma}^{(1)}$. Each raw sample data can be represented as Equation (1).

$$\boldsymbol{\gamma}^{(1)} = (y_1^{(1)}, y_2^{(1)}, ..., y_m^{(1)})^T \tag{1}$$

After sample preprocessing, the input vector A is mapped into a low-dimensional vector, so that the vector length is reduced, that is, the n-dimensional output vector A, which can be expressed as Equation (2).

$$\boldsymbol{\gamma}^{(2)} = (y_1^{(2)}, y_2^{(2)}, ..., y_n^{(2)})^T \tag{2}$$

Input data $\boldsymbol{\gamma}^{(1)}$ is usually original data, which has great difference in dimension and value range, large amount of data and deep hidden data features. Direct application to artificial neural network modeling will lead to long training time, low precision and non-convergence of the model. After data preprocessing, output data $\boldsymbol{\gamma}^{(2)}$ can be obtained, which has a unified value range and complete feature information. It is easy to handle, conducive to the later model training, can speed up the modeling speed, and reduce the model error.

2.2. **Key device of radio frequency circuit.** A complete RF communication system consists of three parts: signal transmitter, receiver, and antenna [24]. After the baseband signal generated by the signal source is input to the transmitter, the electromagnetic signal is radiated outward from the transmitting antenna through modulation, up conversion, power amplification, filtering, etc.; After the electromagnetic wave signal reaches the receiver through the receiving antenna, the signal is processed by demodulation, filtering, low noise amplification, etc., and finally the baseband signal is restored.

The transceiver and reception structures used in RF circuits are different, and their application scenarios are different. Different scenarios and different transceiver structures determine the complexity, performance indicators and power consumption of the transceiver system [25]. As shown in Figure 1, the receiver structure block diagram in the radio frequency electronic communication system: the signal enters the LNA after being received by the receiving antenna, and the signal is amplified and turned on. After filtering through the image filter, and then entering the mixer for mixing, the intermediate frequency signal is obtained and then filtered and amplified to demodulate the original IQ two-way baseband signal.

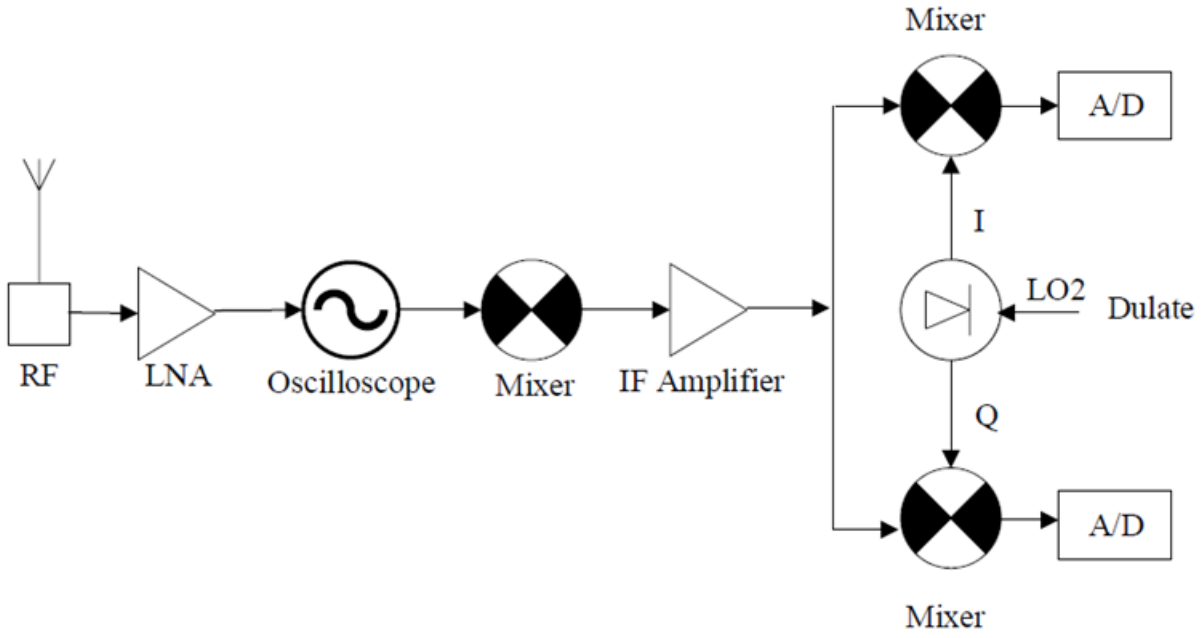

Figure 1. Structure diagram of radio frequency electronic communication system receiver

In this structure, due to the low frequency of the IF signal, the filter Q value required for channel selection in this band is much lower than the filter Q value required when selecting a channel in the RF band, which makes IF filtering easier. In addition, the signal received by the receiving antenna is extremely weak, and the signal needs to be amplified by tens of dB or even hundreds of dB, and if the amplification in the same frequency band is too high, it may cause the amplifier to oscillate. Therefore, the gain index is assigned to the RF, IF and baseband in the superheterodyne structure, which can ensure the stability of the system to a certain extent. In addition to the above characteristics, superheterodyne receivers also have the advantages of large link gain, stable performance, and large dynamic range. On the ground of this feature, and the actual requirements that the RF front-end should have large dynamic range, good reception sensitivity and

implementation complexity, this paper finally chooses this structure as the RF front-end structure of the transceiver.

3. **Intelligent neural network modeling.** This paper proposes an intelligent neural network modeling system, which combines data preprocessing, sample initial value optimization and neural network training and testing process to realize intelligent modeling functions, and the method flow, as shown in Figure **??**, the specific calculation steps are as follows:

Step 1: Sample data preprocessing process. First, in terms of the initial sample data of the RF circuit, the dimensions of the sample input space and output are determined. Then, the initial sample set is normalized and the Pearson correlation coefficient between the different variables and the output response is calculated. If the correlation coefficient is less than the reference value, you can change the variable to a constant. Finally, feature extraction is performed on the data. Using the Gaussian kernel function, the Gaussian kernel matrix of the sample is calculated, and the feature decomposition is carried out to form a mapping matrix, and the sample can be obtained with a high-quality sample by using the mapping matrix to complete the reconstruction of the sample data.

Suppose a neural network mapping from the vector Y of M-dimensional input space to the N-dimensional output space vector X. Given in N-dimensional space, there are many sample data, each sample dataset can be represented as (Y, X), the input vector is Y, and the corresponding target output value in the output space is X. The purpose of building a neural network model is to find a nonlinear mapping function F that can accurately fit all sample data and meet the following mapping conditions:

$$F(Y) = X \tag{3}$$

To build a radial basis neural network model, you need to select Q data center points before training sample data, and construct Q radial basis function functions, which are in the form:

$$F(Y) = \sum_{p=1}^{P} v_p \delta(\|y - y_p\|) + c = \sum_{p=0}^{P} v_p \delta(\|y - y_p\|) \tag{4}$$

Step 2: The optimization process of the initial value of the neural network using the sample. The neural network sample optimization model calculation flow is displayed in Figure 3. First, network initialization. Initialize the structure, activate the function, set the weights and thresholds of the network model to the input variables to be optimized; After that, start initializing parameters d, v, s, etc. The optimal initial value of the neural network is found by continuously optimizing the position of the particle swarm.

Then, the network error is taken as the fitness function, and the error is recorded as the particle adaptation value, and then arranged according to the adaptation value. The best position of individual particles and group particles at this time is found respectively. Finally, determine whether the convergence of the calculation result ends the calculation. If convergence or the maximum number of iterations is reached, the iterative calculation is stopped, so as to complete the learning process of the network weights; Otherwise, proceed to the next velocity and position according to Equation (5) until the solution requirement is completed.

$$\begin{aligned} W_i^{j+1} &= vw_i^j + d_1 * s_1 * (Q_i^j - Y_i^j) + d_2 * (Q_f^s - Y_i^j) \\ Y_i^{j+1} &= Y_i^s + W_i^s \end{aligned} \tag{5}$$

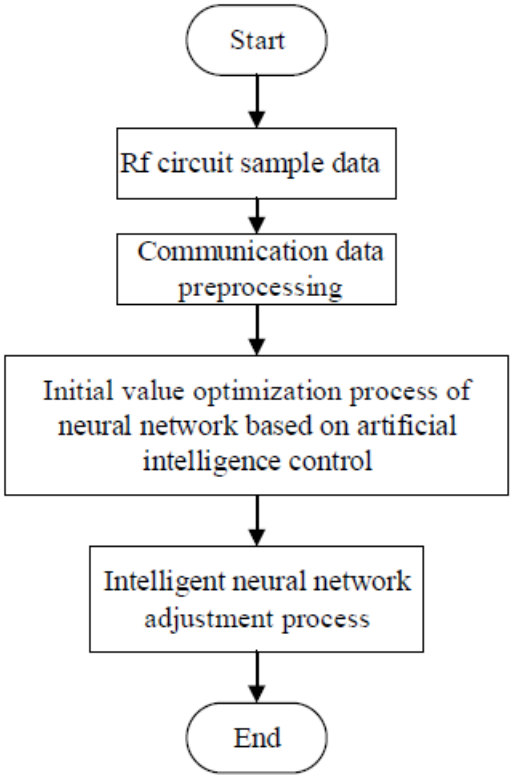

Figure 2. Intelligent neural network modeling flowchart

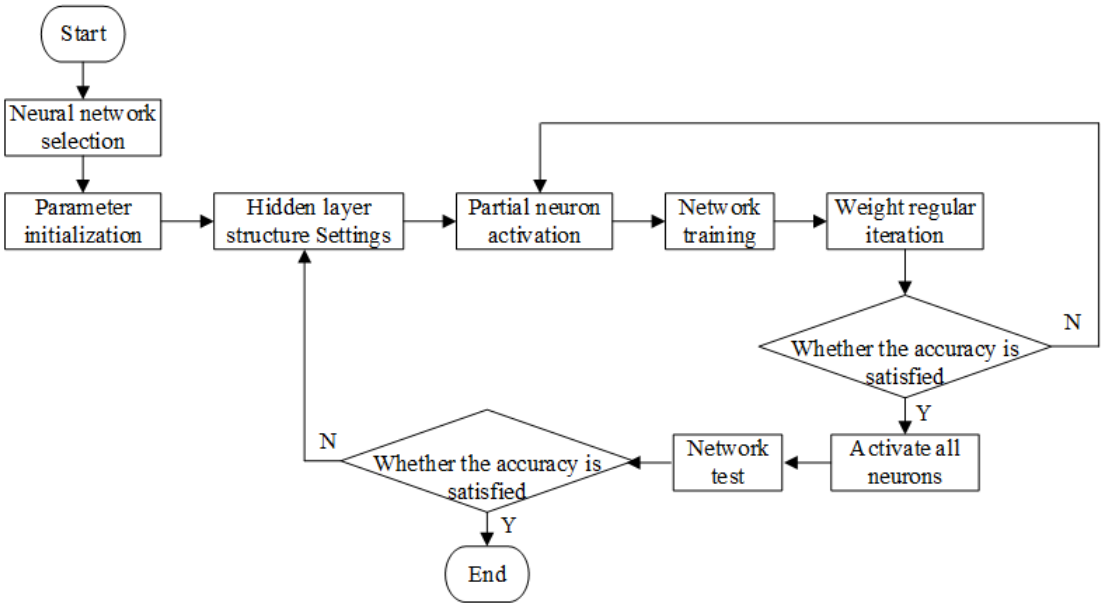

Figure 3. Intelligent neural network modeling optimization flowchart

Step 3: Tune the neural network. To solve the objective function minimum, on the ground of the Lagrangian method, establish the loss function, as shown in Equation (6).

$$F = \frac{1}{2}v^T v + D\sum_{j=1}^{m}\vartheta_j \sum_{j=1}^{n}\beta_j(x_j(v^T(\delta(y_j)+c)-1+\vartheta_j)) \tag{6}$$

When the objective function F takes minimum value, the values obtained by function F for parameters d, v and s are all 0, and the Equation (7) can be obtained.

$$stc : \left\{ \sum_{i=1}^{m} \beta_j x_j = 0, 0 \leq \beta_j \leq D \right. \tag{7}$$

Use the test data to test the neural network, if the test error is less than the expected value, then the neural network model modeling is completed. Otherwise, it indicates that the generalization ability of the neural network is poor, and the system steps need to be automatically entered into Step 2.

4. **Design of radio frequency electronic communication system based on artificial intelligence control.**

4.1. **Module division and function.** The RF electronic communication system model based on artificial intelligence control proposed in this paper is composed of intelligent neural network information source S, off-network relay R that moves randomly in the coverage area of S, and distant (possibly deployed outdoors) destination user U (such as base station, access point, etc.). Considering that the beam is radiated from the light source S, the coverage area of S can be considered to be conical. Suppose that the trunk R moves on the bottom surface of a cone with O as the center and r_1 as the radius.

Since the transceiver channel of the RF electronic communication system adopts the secondary superheterodyne receiving structure and the secondary frequency conversion transmission structure, the design scheme is more complex [26, 27], and based on the equipment module debugging and system scalability considerations, it is necessary to divide the design scheme by module in the design process, on the one hand, there is a good degree of isolation between different modules. It can reduce crosstalk between RF signals and ensure signal quality; On the other hand, it is convenient to locate and deal with faults during the debugging process of the whole machine, and increase the debugging efficiency. The module division and functions of the transceiver channel of the RF subsystem are shown in Table 1, which divides the transceiver channel into four functional submodules: receiving channel, transmission channel, local oscillator and power supply.

Table 1. Division and Function of RF Transceiver Channel Modules

Module Name	**Module Functions**	**Parameter**
Receive link	Selecting useful signals from weak electromagnetic signals	RF 5000MHz ∼ 5300 MHz →Baseband 48 MHz∼ 68 MHz
Transmitting link	Effectively transmitted radio frequency signal	Baseband 48 MHz∼68 MHz → RF 5000 MHz∼ 5300 MHz
Low local oscillator	Baseband and intermediate frequency conversion provide local vibration	LO_L:828 MHz
High local oscillator	IF and RF frequency conversion provide local oscillator	LO_H: 5770 MHz∼ 6050 MHz
Power module	Provides power support for the transceiver channel	18V, 8V, 20V, 5.3 V

4.2. **Radio frequency electronic communication signal transmission.** In a typical indoor scenario, the weakest RF component is at least 7dB higher than the strongest diffuse component [28]. To facilitate the analysis, this paper ignores the multipath reflection in the VLC channel, and only considers the LOS transmission link between the source S and the trunk R. The channel gain of the first hop $S \to R$ can be expressed as:

$$\mathcal{G}_1 = \frac{m+1}{2\pi c_1^2} J_s F_r(\phi) l(\phi) \cos(\phi) \cos^m(\vartheta) \tag{8}$$

where m is the Lambertian radiation coefficient, ϕ is the half power angle of the light source S, $c_1 = \sqrt{f_1^2 + s^2}$ is the length of the direct link from S to R, f_1 is the distance from S to O, S is the distance from O to R, J_s is the effective area of communication, ϕ is the radiation angle of the light source S, and ϑ is the incidence angle, $\phi = \vartheta = \arctan(s/f_1)$.

$F_r(\phi)$ is the gain of the optical filter; $l(\phi) = \zeta^2 / \sin^2(\rho_{f_i e})$ is the optical concentrator gain, where ζ is the refractive index and $\rho_{f_i e}$ is the field of view Angle.

Let $y(s)$ be a modulated source signal with peak amplitude C, and before being used to modulate the RF frequency, DC bias A is added to $y(s)$ to ensure that the resulting signal is non-negative, i.e., $[y(s) + A] \geq 0$. Therefore, the optical signal transmitted by communication can be represented as $y_s^t = Q[y(s) + A]$. Where Q is the transmitting power per unit current on the electric signal $y(s) + A$; $y(s) \in [-C, C]$; $E[y(s)] = 0$, $E[.]$ is the expectation operator.

Combined with the actual situation, in order to ensure the transmission security of the RF electronic communication system, the average power and peak power constraints must be met at the same time [29], as shown in:

$$\begin{aligned} &E[y(s)] \leq Q_c \Rightarrow A \leq \frac{Q_C}{Q} \\ &0 \leq y(s) \leq Q_{\max} \Rightarrow C \leq \min\left\{A, \frac{Q_{\max}}{Q} - A\right\} \end{aligned} \tag{9}$$

In the equation, Q_c and $Q_{\max}$ are the maximum allowable average power and peak power of the source respectively.

4.3. **Radio frequency electronic communication signal transmission.** On the ground of the above signal transmission, the communication signal received by Relay R can be expressed as:

$$x_t(s) = \alpha f_1 y_r(s) + m_1(s) = \alpha f_1 Q y(s) + \alpha f_1 Q A + m_1(s) = x_{ac}(s) + x_{dc} + m_1(s) \tag{10}$$

In the equation, $x_{ac}(s) = \alpha f_1 Q y(s)$ is the responsiveness, $x_{dc} = \alpha f_1 Q A$ is the AC component, and $x_{dc} = \alpha f_1 Q A$ is the DC component.

In addition to receiving the LOS signal from the light source S, the relay R will also receive the ambient light from other light sources. After sufficient reflection, refraction and scattering, the ambient light will reach R through different paths, so that it has different arrival angles, different delays or phases, and different amplitudes. In other words, ambient light noise is the superposition of a large number of statistically independent random variables. Then, in terms of the central limit theorem, $m_1(s)$ is the total noise generated by the superposition of ambient visible light, background lens noise, and thermal noise, and $m_1(s) \sim \mathcal{A}_{\mathrm{CN}}(0, \theta_1^2)$.

Relay R splits the received photocurrent into two parts by employing signal component segmentation: an AC component for information decoding and a DC component for energy harvesting. The energy collected can be expressed as:

$$E = g x_{dc} T_{oc} = g \alpha f_1 Q A T_v \ln(1 + \frac{\alpha f_1 Q A}{J_0}) \approx \frac{g T_v (\alpha Q A)^2 \mu_1}{J_0} \tag{11}$$

where the filling factor g is between 0.5 and 1, T_{oc} is the open circuit voltage of communication, and J_0 is the saturated dark current. Equation (11) is an approximate expression obtained by using $\alpha f_1 QA \to 0$ when $\ln(1 + \alpha f_1 QA/J_0) \approx (\alpha f_1 QA/J_0)$.

If $\mu_1 = |f_1|^2$, the Equation (12) is obtained, where $l = [F_s T_r(\phi)h(\phi)]/2\pi$ is a constant.

$$\mu_1 = \frac{[(m+1)f_1^{m+1}]^2}{(l^2 + f_1^2)^{m+3}} \tag{12}$$

On the other hand, the relay R will attempt to recover the source signal $y(s)$ from the AC component $x_{ac}(s)$. If R can successfully decode the source signal C, it uses the energy collected from the DC component x_{ac} to forward the decoded signal to the destination user D; otherwise, the communication is interrupted.

5. **System performance test and analysis.**

5.1. **Transmit channel output power test.**

To verify the performance of the system, this paper uses Python V3.9 to analyze and simulate the performance evaluation of the RF electronic communication system on the ground of artificial intelligence control, and compares the performance of the existing RF electronic communication system [30] based on hybrid collaboration. The radio frequency electronic communication system designed in this article is denoted OUR. This paper comprehensively considers the random movement characteristics of relay R, the information decoding state of R, the energy harvesting state of R, and the energy harvesting state of R. The complex fluctuation characteristics of the channel during a two-hop transmission due to random mobility. Data transmission flow of the intelligent communication transceiver used in the simulation experiment in this section is shown in Figure 4.

The output power is the most important indicator of the transmitter, which determines the transmission distance of the low-frequency baseband signal modulated by the wireless communication system to the radio frequency band. After power-on, signal source 1 outputs 20 MHz as an external reference clock, and signal source 2 inputs 38MHz single-tone signals with a power of about 0dBm. The PC controls the FPGA output control word through the JTAG interface to configure the internal register sets of SI4133 and ADF4355. The low local SI4133 outputs a fixed 828MHz signal, and the high local ADF4355 outputs a total of 10 frequency points of 5770MHz∼6050MHz signal, respectively. The spacing of each frequency point is 20MHz, respectively representing the input third-order intercept IIP3 of the output power mixer MIX2 of the 15 transmission channels is +7dBm, while the input power of the IF port of MIX2 is 760MHz∼780MHz under the control of the attenuator PE402 is -17.5dBm∼14dBm. In order to avoid the input power exceeding +7dBm working in the nonlinear region, the PE4302 attenuation is 10dB controlled by the PC. The spectrometer is connected to the antenna input port SMA of the transmitting channel through the coaxial line to record the test results, as shown in Figure 5. The spectrum test diagram of 5140MHz single tone output by RF channel 8 is shown in Figure 6.

As can be seen from Figure 6, when the channel is located at 5, the transmitting channel power of the system designed in this paper is 10.6dBm, and the ABDN power is 15.5 dBm. The output power of the 10 channels of the upper transmission channel is greater than 14dBm, which meets the output power requirements of the transmission link. However, the output power budget of the entire transmission channel is about 19dBm when the attenuation attenuates 10dB, and the difference between the measured value and the budget design value is about 3dB. The overall trend is that the closer the middle channel is, the smaller the gain flatness is, because the middle channel is close to the center frequency of the band preselected filter 5150MHz, and the edge channel is just

close to the edge of the pre-gated band. This will lead to a certain deterioration in gain flatness. Overall, the gain flatness of the transmitting channel is less than 1.5dB, which meets the requirements of the design index.

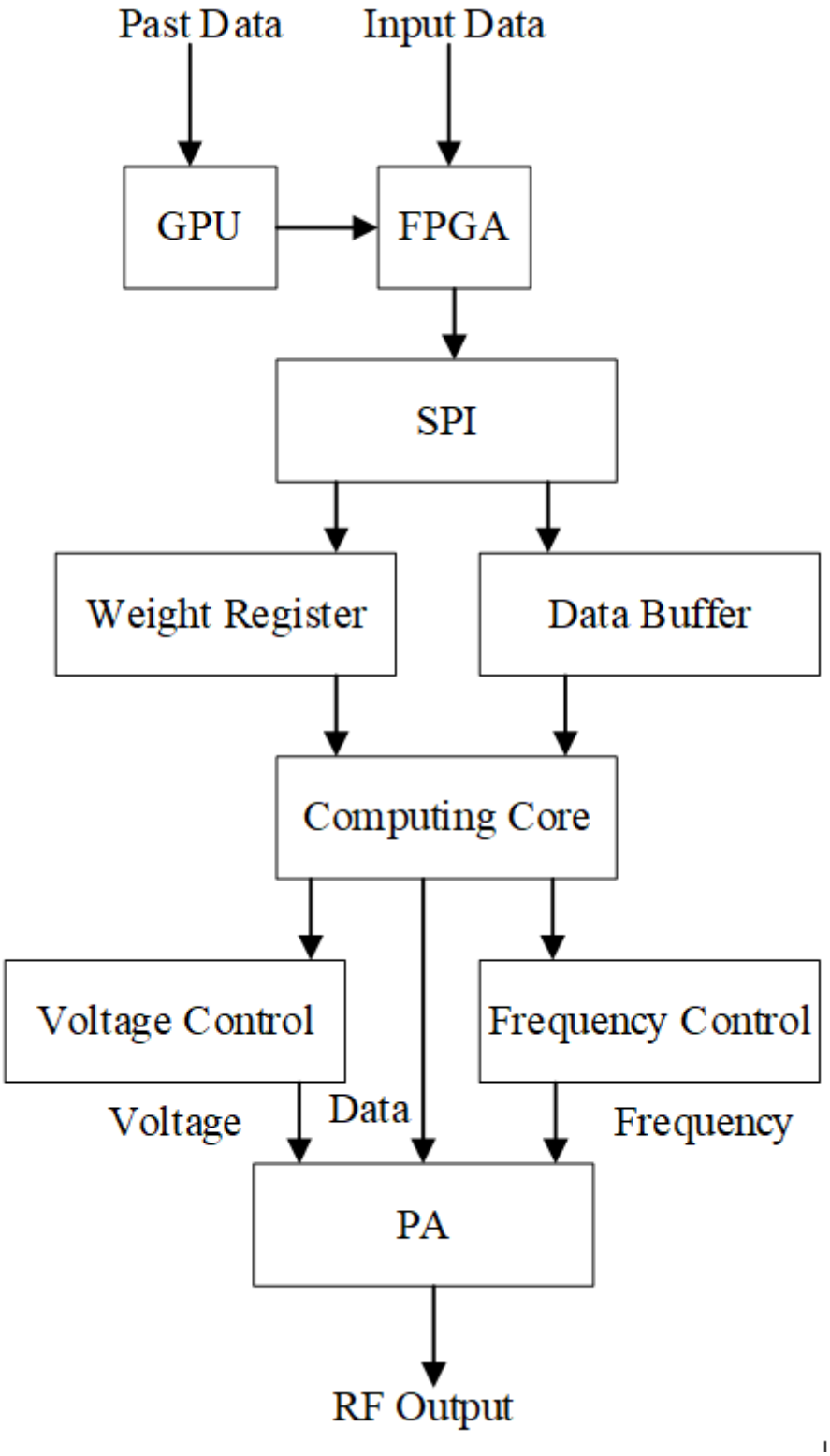

Figure 4. Data transmission flow of intelligent communication transceiver

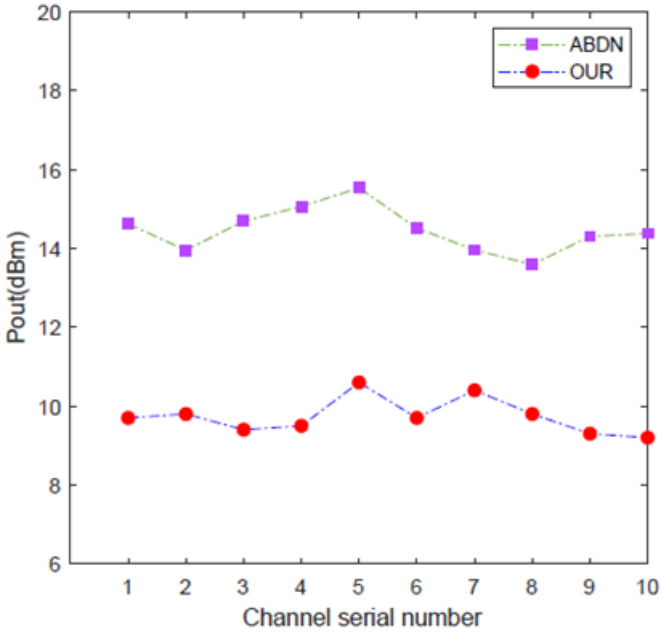

Figure 5. Transmission channel output power comparison

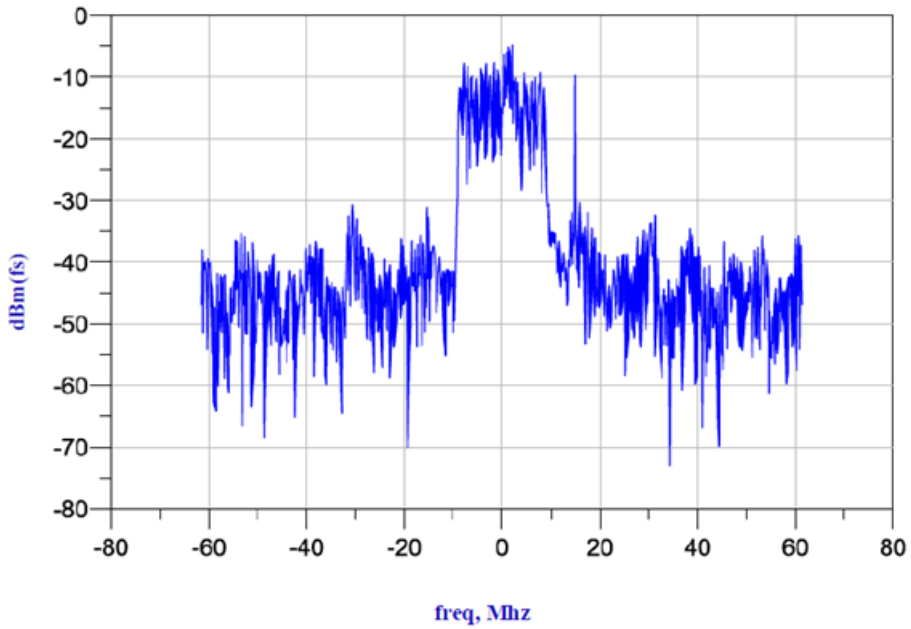

Figure 6. Power gain flatness of the transmit channel

5.2. **Transmit channel output power test.** For the optimized RF electronic communication system, modulation accuracy EVM is a key indicator to reflect the system performance, on the one hand, it can characterize the system modulation and demodulation performance, measure the distortion degree of the in-band signal, and on the other hand, it also indirectly reflects the influence of various RF defects of the system on the modulation accuracy. This article looks at the EVM test results for two different modulation types of a dual-channel receiver, and the final test results are shown in Table 2.

As can be seen from Table 2, when the channel is 1 and the bitrate is set to 100, the modulation accuracy and error tolerance rate (Err) of the OUR system, frequency, offset

are better than ABDN system. The EVM shown in the following table characterizes the modulation accuracy of the channel transmitter, considering the 1dB loss of the receiver's transceiver switch and the 1dB loss of the receiver-test instrument's cable. Comparing the system design requirements with the actual test results, it can be seen that the test results all meet the transmitter requirements.

Table 2. EVM test results of two-channel transmitter

Modulation type	**Bit rate (Mbps)**	**EVM (%ms)**	**Err (%ms)**	**Freq (kHz)**	**IQ offset (dB)**
Ch1-ABDN	100	1.8976	1.6429	1.9732	-78.439
Ch1-OUR	100	1.6743	1.4982	1.6592	-43.975
Ch2-ABDN	100	1.7821	1.7399	1.7834	-85.573
Ch2-OUR	100	1.4972	1.3768	1.4875	-58.328

5.3. **System gain flatness test.** After power-on, the PC side controls the FPGA output control word, so that the low local oscillator is fixed to generate 828MHz and the high local oscillator generates 5910MHz (channel 8) respectively. Meanwhile, signal source 2 outputs 48MHz to 68MHz signals with a sweep frequency spacing of 0.01MHz. Similarly, the Max hold function of the spectrometer is used to measure the gain flatness curves of the mixer MIX1 input 760MHz 780MHz and the low-frequency 48MHz 68MHz after loopback, as shown in Figure 7. As can be seen from the test curve, when the channel is 8, the gain flatness of the system designed in this paper is 1.8dB, and the ABDN is 4.5dB. After the frequency band response of down-conversion and post-amplification filtering, the flatness of 48MHz 68MHz signal output to the baseband subsystem is 1.49dB. Therefore, the RF electronic communication system optimized in this paper has lower system gain flatness, better than ABDN, and meets the performance requirements.

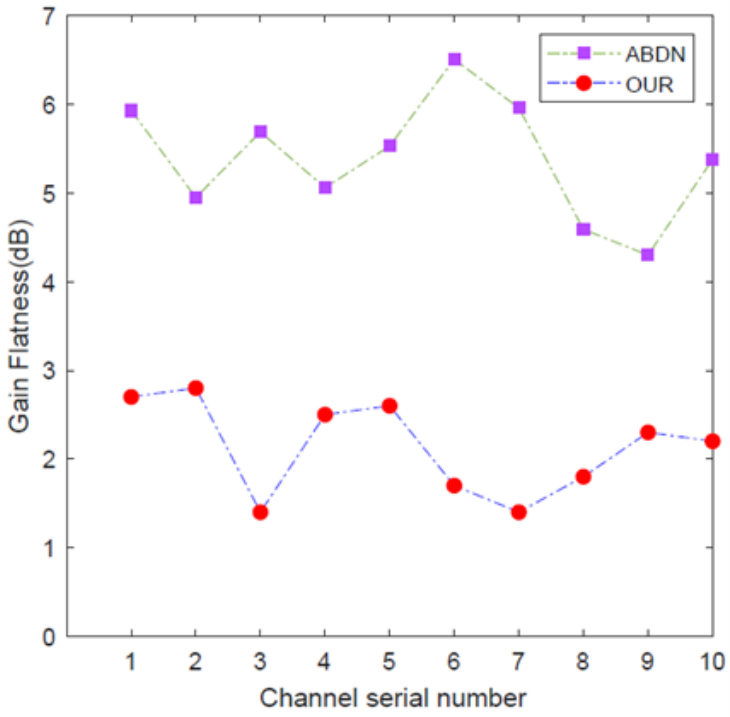

Figure 7. System gain flatness comparison

As shown in Figure 8, we can see that the power gain flatness of the 10 channels in the 5000MHz–5300MHz operating band is less than 2.5dB, and the power gain flatness near the passband edge of the band preselected filter is worse than that of the middle channel, which meets the index requirement of the system power gain flatness less than 3dB.

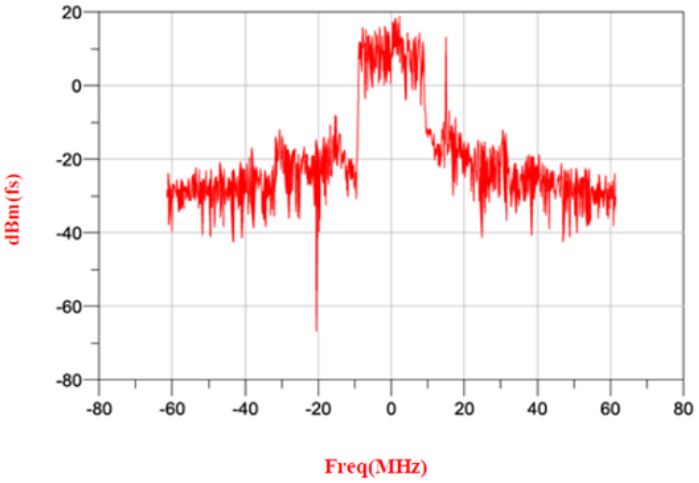

Figure 8. System power gain flatness

6. **Conclusion.** In this paper, on the basis of artificial intelligence neural network control method, the establishment of a high-performance RF electronic communication system is studied. Firstly, in the process of data preprocessing, a data conversion method is designed, which combines Pearson correlation coefficient to quantify the correlation degree between input variables and output responses, and can exclude input variables unrelated to output responses. Then the secondary superheterodyne receiving structure and the secondary frequency conversion transmitting structure are used to divide different modules according to the current to ensure the isolation between the modules and reduce the crosstalk between the RF signals, thus improving the communication efficiency. Finally, the experimental results show that the optimized system can effectively reduce the system gain flatness, modulation accuracy, and power gain flatness.

Acknowledgment.

1. The Science and Technology Re-search Project of Chongqing Education Commission (No. KJQN202203213 ,No. KJQN202403214, No.KJZD-K202403206).

2. Technology Innovation and Application Development Shandong-Chongqing Science and Technology Cooperation Special Project of Chongqing Science and Technology Bureau (No.CSTB2024TIAD-LDX0019).

REFERENCES

[1] D. Todolí-Ferrandis, J. Silvestre-Blanes, S. Santonja-Climent, V. Sempere-Paya, and J. Vera-Pérez, "Deploy&Forget wireless sensor networks for itinerant applications," *Computer Standards & Interfaces*, vol. 56, pp. 27-40, 2018.

[2] T. Li, Y. Dong, P. Fan, and K. B. Letaief, "Wireless communications with RF-based energy harvesting: From information theory to green systems," *IEEE Access*, vol. 5, pp. 27538-27550, 2017.

[3] B. Liu, D. Zhao, P. Reynaert, and G. G. Gielen, "Synthesis of integrated passive components for high-frequency RF ICs based on evolutionary computation and machine learning techniques," *IEEE Transactions on Computer-Aided Design of Integrated Circuits and Systems*, vol. 30, no. 10, pp. 1458-1468, 2011.

[4] A. C. W. Wong, G. Kathiresan, C. K. T. Chan, O. Eljamaly, O. Omeni, D. McDonagh, A. J. Burdett, and C. Toumazou, "A 1 V wireless transceiver for an ultra-low-power SoC for biotelemetry applications," *IEEE Journal of Solid-State Circuits*, vol. 43, no. 7, pp. 1511-1521, 2008.

[5] Y.-J. Kim, H. S. Bhamra, J. Joseph, and P. P. Irazoqui, "An ultra-low-power RF energy-harvesting transceiver for multiple-node sensor application," *IEEE Transactions on Circuits and Systems II: Express Briefs*, vol. 62, no. 11, pp. 1028-1032, 2015.

[6] J. E. Rayas-Sánchez, F. Lara-Rojo, and E. Martínez-Guerrero, "A linear inverse space-mapping (LISM) algorithm to design linear and nonlinear RF and microwave circuits," *IEEE Transactions on Microwave Theory and Techniques*, vol. 53, no. 3, pp. 960-968, 2005.

[7] P. Sen, W. H. Woods, S. Sarkar, R. J. Pratap, B. M. Dufrene, R. Mukhopadhyay, C.-H. Lee, E. F. Mina, and J. Laskar, "Neural-network-based parasitic modeling and extraction verification for RF/millimeter-wave integrated circuit design," *IEEE Transactions on Microwave Theory and Techniques*, vol. 54, no. 6, pp. 2604-2614, 2006.

[8] V. Chandrasekaran and M. I. Jordan, "Computational and statistical tradeoffs via convex relaxation," *Proceedings of the National Academy of Sciences*, vol. 110, no. 13, pp. 1181-1190, 2013.

[9] H. Kabir, Y. Wang, M. Yu, and Q.-J. Zhang, "High-dimensional neural-network technique and applications to microwave filter modeling," *IEEE Transactions on Microwave Theory and Techniques*, vol. 58, no. 1, pp. 145-156, 2009.

[10] Y. Ko, P. Roblin, A. Zárate-de Landa, J. A. Reynoso-Hernandez, D. Nobbe, C. Olson, and F. J. Martinez, "Artificial neural network model of SOS-MOSFETs based on dynamic large-signal measurements," *IEEE Transactions on Microwave Theory and Techniques*, vol. 62, no. 3, pp. 491-501, 2014.

[11] Y. Tian, N. Li, H. Wang, X. P. Li, and K. Y. Lee, "Right-angled microcoaxial bends for Si-based RF/microwave integrated circuits," *IEEE Transactions on Components, Packaging and Manufacturing Technology*, vol. 6, no. 2, pp. 290-297, 2016.

[12] N. Srivastava, G. Hinton, A. Krizhevsky, I. Sutskever, and R. Salakhutdinov, "Dropout: a simple way to prevent neural networks from overfitting," *The Journal of Machine Learning Research*, vol. 15, no. 1, pp. 1929-1958, 2014.

[13] F. Inanlou, M. Kiani, and M. Ghovanloo, "A 10.2 Mbps pulse harmonic modulation based transceiver for implantable medical devices," *IEEE Journal of Solid-State Circuits*, vol. 46, no. 6, pp. 1296-1306, 2011.

[14] H. B. Kia, "A High Gain and Low Noise Amplifier Design Using New Noise Canceling Technique for Wireless Receivers," *The Journal of Telecoms Engineering Letters*, vol. 3, no. 1, pp. 36–42, 2018.

[15] X. Lu, P. Wang, D. Niyato, D. I. Kim, and Z. Han, "Wireless networks with RF energy harvesting: A contemporary survey," *IEEE Communications Surveys & Tutorials*, vol. 17, no. 2, pp. 757-789, 2014.

[16] U. Rosenberg, M. Salehi, J. Bornemann, and E. Mehrshahi, "A novel frequency-selective power combiner/divider in single-layer substrate integrated waveguide technology," *IEEE Microwave and Wireless Components Letters*, vol. 23, no. 8, pp. 406-408, 2013.

[17] K.-L. Wu, K.-T. Lai, R. Hu, C. F. Jou, D.-C. Niu, and Y.-S. Shiao, "77–110 GHz 65-nm CMOS power amplifier design," *IEEE Transactions on Terahertz Science and Technology*, vol. 4, no. 3, pp. 391-399, 2014.

[18] J. Joung, C. K. Ho, K. Adachi, and S. Sun, "A survey on power-amplifier-centric techniques for spectrum-and energy-efficient wireless communications," *IEEE Communications Surveys & Tutorials*, vol. 17, no. 1, pp. 315-333, 2014.

[19] Y. Song, R. Zhu, and Y. E. Wang, "An X-Band Pulsed Load Modulation Transmitter with Multilevel Envelope Delta–Sigma Modulations," *IEEE Transactions on Microwave Theory and Techniques*, vol. 64, no. 11, pp. 3643-3653, 2016.

[20] T. Wu, X. Guo, Y. Chen, S. Kumari, and C. Chen, "Amassing the Security: An Enhanced Authentication Protocol for Drone Communications over 5G Networks," *Drones*, vol. 6, no. 1, 10, 2021.

[21] L. Yang, Y.-C. Chen, and T.-Y. Wu, "Provably Secure Client-Server Key Management Scheme in 5G Networks," *Wireless Communications and Mobile Computing*, vol. 2021, pp. 1-14, 2021.

[22] Y. Ma, Y. Peng, and T.-Y. Wu, "Transfer learning model for false positive reduction in lymph node detection via sparse coding and deep learning," *Journal of Intelligent & Fuzzy Systems*, vol. 43, no. 2, pp. 2121-2133, 2022.

[23] C.-M. Chen, Y. Gong, and J. M.-T. Wu, "Impact of Technical Indicators and Leading Indicators on Stock Trends on the Internet of Things," *Wireless Communications and Mobile Computing*, vol. 2022, pp. 1-15, 2022.

[24] C.-M. Chen, S. Lv, J. Ning, and J. M.-T. Wu, "A Genetic Algorithm for the Waitable Time-Varying Multi-Depot Green Vehicle Routing Problem," *Symmetry*, vol. 15, no. 1, 124, 2023.

[25] J. Hur, H. Kim, O. Lee, K.-W. Kim, F. Bien, K. Lim, C.-H. Lee, and J. Laskar, "A multilevel class-D CMOS power amplifier for an out-phasing transmitter with a nonisolated power combiner," *IEEE Transactions on Circuits and Systems II: Express Briefs*, vol. 63, no. 7, pp. 618-622, 2016.

[26] S. H. Scheres, and S. Chen, "Prevention of overfitting in cryo-EM structure determination," *Nature Methods*, vol. 9, no. 9, pp. 853-854, 2012.

[27] R.-F. Ye, T.-S. Horng, and J.-M. Wu, "Low power FSK receiver using an oscillator-based injection-locked frequency divider," *IEEE Microwave and Wireless Components Letters*, vol. 24, no. 2, pp. 114-116, 2013.

[28] H. Jin, D. Kim, and B. Kim, "Efficient digital quadrature transmitter based on IQ cell sharing," *IEEE Journal of Solid-State Circuits*, vol. 52, no. 5, pp. 1345-1357, 2017.

[29] A. Paidimarri, N. Ickes, and A. P. Chandrakasan, "A+ 10 dBm BLE transmitter with sub-400 pW leakage for ultra-low duty cycles," *IEEE Journal of Solid-State Circuits*, vol. 51, no. 6, pp. 1331-1346, 2016.

[30] Z. Liu, X. Hu, T. Liu, X. Li, W. Wang, and F. M. Ghannouchi, "Attention-based deep neural network behavioral model for wideband wireless power amplifiers," *IEEE Microwave and Wireless Components Letters*, vol. 30, no. 1, pp. 82-85, 2019.